AD NUMBER: AD0019206

LIMITATION CHANGES

TO:

Approved for public release; distribution is unlimited.

FROM:

Distribution authorized to US Government Agenncies and their contractors; Administrative/Operational Use; 4 Feb 1953. Other requests shall be referred to US Naval Ordnance Laboratory, White Oak, MD 20904.

AUTHORITY

USNOL ltr dtd 29 Aug 1974

NAVORD REPORT 2774

BASE PRESSURE OF SPHERES AT SUPERSONIC SPEEDS

4 FEBRUARY 1953

U. S. NAVAL ORDNANCE LABORATORY
WHITE OAK, MARYLAND

BASE PRESSURE OF SPHERES AT SUPERSONIC SPEEDS

Prepared by:

Richard Lehner

ABSTRACT: Base-pressure measurements on spheres with various diameters were carried out at Mach numbers between 1.57 and 5.0 in the NOL 40 x 40 cm Aeroballistics Wind Tunnels No. 1 and No. 2 to study Mach number and Reynolds number effects in a Reynolds number region between approximately 10^5 and 10^6.

The base-drag coefficient was determined from measured base-pressure data and coordinated flow separation locations taken from schlieren photographs. The behavior of the base-drag coefficient is discussed in comparison with the calculated wave-drag coefficient and existing data of the total-drag coefficient.

Flow-separation phenomena found to be departing from those at subsonic speeds are briefly analyzed.

The failure in detecting Reynolds number effects by previous total-drag measurements can be explained by the small contribution of the base-drag component to the total-drag at supersonic speeds.

U. S. NAVAL ORDNANCE LABORATORY
WHITE OAK, MARYLAND

NAVORD Report 2774 4 February 1953

The material presented here represents additional basic information on the general subject of base pressure of bodies at supersonic speeds.

Experimental data were obtained during the calendar years of 1950, 1951, and 1952 at the U. S. Naval Ordnance Laboratory. This work was sponsored by the Navy Bureau of Ordnance under task number NOL-Re9a-108.

The author is indebted to H. H. Kurzweg and G. R. Eber for their comments on the problem and S. M. Hastings, M. O'Brien, E. Redman, R. Lee, and Martha Jennison for their help on the experiments in the wind tunnel, the evaluation of wind-tunnel tests and the computation of the wave drag. Thanks are due A. May and W. R. Witt, Jr. for the use of shadowgraphs taken in the NOL Pressurized Ballistics Range.

EDWARD L. WOODYARD
Captain, USN
Commander

H. H. KURZWEG
Aeroballistic Research Department
By direction

CONTENTS

ILLUSTRATIONS

SYMBOLS

M	=	Mach number
Re	=	Free-stream Reynolds number referred to sphere diameter
α	=	Angle of attack of support sting
D	=	Sphere diameter
d	=	Sting diameter
p_b	=	Base pressure
p_a	=	Ambient static pressure
$\frac{p_b}{p_a}$	=	Base-pressure ratio
C_{D_t}	= $\frac{D_t}{qA}$ =	Total-drag coefficient; D_t = Total drag
C_{D_w}	= $\frac{D_w}{qA}$ =	Wave-drag coefficient; D_w = Wave drag
C_{D_b}	= $\frac{D_b}{qA}$ =	Base-drag coefficient; D_b = Base drag
q	= $\frac{\rho V^2}{2}$ =	Dynamic pressure
A	= $\frac{\pi D^2}{4}$ =	Frontal area
ρ	=	Density
V	=	Velocity

BASE PRESSURE OF SPHERES AT SUPERSONIC SPEEDS

INTRODUCTION

1. The simplicity of its shape helped the sphere to become a classical model for aerodynamic and ballistic investigations. Since the famous investigations carried out by Eiffel at Paris and Prandtl at Goettingen (1910 - 1912) (a) the sphere has been a standard model for very conclusive studies of aerodynamic problems. The sphere was also frequently used for studies of measuring techniques in wind tunnels and firing ranges. Last, but not least, the sphere became an indicator of the degree of turbulence of subsonic wind tunnels due to its critical behavior at a Reynolds number of about 250000.

2. The early development of supersonic wind-tunnel techniques tried to take advantage of the characteristic features of the sphere found at subsonic speeds. The most striking problem, of course, was the study of Reynolds number effects in general and specifically the possible detection of a critical Reynolds number at supersonic speeds. The oldest known attempt to study Reynolds number effects on spheres at supersonic speeds was made by A. Eula at Guidonia, Italy (b). It was shown at Mach numbers of $M = 1.85$ and $M = 2.13$ that the total-drag coefficient is invariant with Reynolds number in a Reynolds number region between 10^5 and 8×10^5. Later investigations carried out almost simultaneously by O. Walchner at Goettingen, Germany (c) at Mach numbers between 1.2 and 3.2, and by the author at Peenemuende, Germany (d) at Mach numbers between 1.2 and 4.3, confirmed A. Eula's results. Even more recent investigations of the drag and the flow pattern of spheres by A. C. Charters and R. N. Thomas (e) failed to detect a critical Reynolds number or a systematic Reynolds number effect at supersonic speeds, in general, within a considered Reynolds number region between about 0.4×10^6 and 1.3×10^6.

OBJECTIVE

3. The immediate objective was the determination of the base pressure in connection with a systematic

investigation of the relationship between boundary layer and base-pressure behavior carried out at the Naval Ordnance Laboratory, White Oak, Maryland. Among other axially-symmetrical models the sphere was chosen as a basic representative of a blunt test model.

4. Since particular information regarding the Reynolds number effect on the overall aerodynamic performance of spheres at supersonic speeds was considered desirable it was decided not to concentrate on the base pressure only but also to take into consideration the wake flow study and a comparison between base drag-, wave drag- and total-drag coefficient.

EQUIPMENT AND PROCEDURE

5. The investigations were carried out in the 40 x 40 cm Aeroballistics Tunnels No. 1 and No. 2 of the Naval Ordnance Laboratory which are described in reference (f). Eight smooth steel spheres with the diameters of 0.7925, 0.9515, 1.977, 3.170, 3.959, 5.048, 5.972, and 10.146 cm and a laminated mahogany sphere with a diameter of 19.99 cm were used as models in order to cover a Reynolds number region between about $Re = 0.06 \times 10^6$ and $Re = 1.4 \times 10^6$ at Mach numbers between 1.57 and 5.0. The deviation of the sphere diameters from the given mean values was within 0.01% for the steel spheres and within 0.06% for the wooden sphere.

6. Since the investigation was originally connected with a dynamic test of a three-component external wind-tunnel balance, a split-sting model support was used during part of the investigation. A schematic sketch of the support is shown in Figure 1. For this investigation the length of the split-sting support was arranged so that the sphere center coincided with the center of rotation of the angle of attack mechanism. A one-millimeter gap was left between the front of the tare sting and the model as well as between the tare sting and the model sting. The ratio between the frontal areas of the spheres and their individual supporting split-stings was kept constant at $\frac{D}{d} = 10$

for all cases. This ratio resulted as a safe minimum from the author's previous investigations reported in reference (d). Smaller ratios caused sting interference. The base pressure was taken at a tap located at the flat front of the tare sting as shown in Figure 1.

7. Butyl-Phthalate manometers were used to measure the base pressure with an accuracy of ± 0.1 mm Hg. In general, the investigation was carried out with the support sting at an angle of attack of $\alpha = 0$. In some selected cases the angle of attack of the sting was varied between $\alpha = -6^{o}$ and $\alpha = +9^{o}$.

8. The effect of mechanical boundary-layer disturbances (tripping ring at 25 per cent sphere depth) was studied at one Mach number in order to have a supersonic comparison to Prandtl's classical test at subsonic speeds (a). During one of the early test series the support effect was investigated by replacing the tare sting by a thin copper pipe for the base-pressure measurement. Results of the support effect study are discussed in the appendix. They led to the conclusion to carry out the whole investigation without a tare sting. Schlieren pictures were taken simultaneously with the base-pressure measurements throughout the entire investigation to enable flow structure observation.

RESULTS AND DISCUSSION

9. The results of the base-pressure measurements are presented in Figure 2 as base-pressure ratio p_b/p_a vs. Reynolds number with Mach number as parameter. In the Mach number region from $M = 1.57$ to $M = 3.26$ a common tendency is obvious, i.e., the decrease of the base-pressure ratio with increasing Reynolds number. The average pressure ratio p_b/p_a drops from 0.65 at $Re = 0.06 \times 10^6$ to almost 0.4 at $Re = 1.4 \times 10^6$ and shows a tendency which is characteristic for the base-pressure behavior of axially-symmetrical bodies at supersonic speeds in the investigated region of Reynolds numbers. A comparison with base-pressure data of cone-cylinder models is given in Figure 3. The curves presented are based on experimental findings as reported by H. H. Kurzweg (NOL) in reference (g), Dean R. Chapman (NACA) in reference (h), and S. M. Bogdonoff (Princeton) in reference (i). The referenced data in the Reynolds number region covered by the sphere investigation could

be correlated with the existence of laminar boundary layer over the entire model length. Schlieren photographs of the spheres indicate that laminar boundary layer and laminar flow separation existed at all phases of the investigation. One set of schlieren photographs at a Mach number of M = 3.26 is given in Figures 4a and 4b as an example demonstrating the behavior of the wake flow shape as a function of Reynolds number. The dimensionless wake length decreases with decreasing base pressure in accordance with findings on cone-cylinder models. The wake length variation with Reynolds number was determined by measuring the distance between trailing shock and sphere base in sphere diameters. The trailing shock location was defined as the intersection between the average slopes of the wake and of the trailing shock. The results are given in Figure 5. It appears that the emanation region of the trailing shock moves from about 1.7 sphere diameters behind the rear stagnation point to about 0.7 sphere diameters in a Reynolds number region between 0.05×10^6 and 1×10^6. This tendency is common to all Mach numbers between M = 2.48 and M = 3.26 where schlieren pictures could be properly evaluated. Evaluation of photographs at lower and higher Mach numbers was either obstructed by the strong Mach line pattern or rather low density, respectively. The variation of the dimensionless wake length with Reynolds number shows a tendency that agrees completely with the tendency of the base-pressure ratio variation with Reynolds number in the considered Reynolds number region. This relationship between wake length and base pressure still holds in the case of artificially-disturbed boundary layer as demonstrated by the results from trigger-ring-fitted spheres at M = 2.86 denoted by flagged symbols in Figures 2 and 5. The results show that artificial boundary-layer disturbances can reduce laminar base pressures to values that correspond to a naturally-developed boundary layer at higher Reynolds numbers. Such boundary-layer disturbances do not necessarily cause a base-pressure reduction to the turbulent value if, for instance, the disturbance is applied in a Reynolds number region where the laminar boundary layer is stable enough to prevent immediate transition. However, a change in the profile takes place and, consequently, the base pressure and the wake shape will be affected.

10. The schlieren photographs were not clear enough to obtain numerical data on transition in the mixing zone of

the wake. Fortunately, some useful shadowgraphs from free-flight determinations of the drag coefficient of spheres in the NOL Pressurized Ballistics Range were made available to the author by the courtesy of A. May and W. R. Witt, Jr. (j). For the purpose of comparison with wind-tunnel data the dimensionless wake length was determined from eleven rounds of 1/2 inch and 3/4 inch smooth, steel spheres at Mach numbers between 1.78 and 4.44 covering a Reynolds number region from 0.2×10^6 to 1×10^6. The Reynolds number variation in the firing range was achieved by ambient pressure variation from 184 mm Hg to 760 mm Hg. The dimensionless wake lengths are plotted in terms of distance between trailing shock and sphere base (in sphere diameters) vs. Reynolds number in Figure 5. The data are independent of Mach number and agree well with the wind-tunnel results. Therefore, it can be concluded that the base-pressure behavior at comparable Mach numbers (2.48 to 3.26) is the same for both the wind-tunnel and the firing-range sphere tests in the considered Reynolds number region. Two representative pictures of the various shadowgraphs used for the comparative wake length determination are shown in Figure 6. The long wake length at a lower Reynolds number is clearly distinguished from the short wake length at the maximum Reynolds number observed.

11. The negatives of most of the available shadowgraphs permitted the determination of the location of transition in the mixing zone of the wake. The results are presented in Figure 7 as wake transition distance from the sphere base (rear "stagnation point") in sphere diameters as a function of Reynolds number. The Mach number varied from $M = 2.08$ to $M = 4.44$. However, the Mach number variation does not seem to have any effect on the transition location. Transition in the mixing zone travels from about 1.2 diameters behind the sphere base at $Re = 0.07 \times 10^6$ to a distance of 0.14 diameters at $Re = 1.013 \times 10^6$. The rapid forward motion of transition with increasing Reynolds number in the lower part of the considered Reynolds number region ($0.07 \times 10^6 \leqq Re \leqq 0.4 \times 10^6$) is accompanied by an appreciable decrease of the base-pressure ratio (see Figure 2). The rate of travel of transition with increasing Reynolds number decreases considerably more as transition approaches the sphere (Figure 7), and the base-pressure ratio

decreases correspondingly slower (Figure 2). This observation is in good agreement with the tendency of transition motion in the mixing zone of the wake as theoretically predicted by L. Crocco and L. Lees for the qualitatively similar case of a two-dimensional airfoil with a blunt trailing edge (reference k). According to Crocco and Lees the laminar mixing rate and the transition location in the wake depend upon the model Reynolds number. In the considered Reynolds number region Crocco and Lees explain the decrease of base pressure with increasing Re by the large increase in local mixing rate due to the upstream motion of transition in the wake. The turbulent mixing coefficient is 5 to 10 times large. than the laminar coefficient. The mixing coefficient k has been defined by the relation

$$\frac{d\bar{m}}{dx} = K \varrho_e U_e$$

where $\bar{m} = \int_0^\delta \varrho U \, dy$, the mass flux

ϱ_e = density

U_e = velocity

} at $y = \delta$ and

δ = thickness of the dissipative flow region, in this case the mixing zone of the wake.

From this explanation it can be concluded that the rate of change in base pressure depends upon the rate of travel of transition in the wake with Re variation - which is experimentally shown by the results in Figures 2 and 7.

12. The base-pressure ratio at Mach numbers of M = 4.24 and M = 5.0 does not follow the tendency which was found to be common for Mach numbers between 1.57 and 3.26 with respect to Reynolds number variation. It is known from former base-pressure investigations on cone-cylinder models that the velocity profile as well as the temperature profile in the boundary layer is a determining parameter for the base pressure. The temperature profile is dependent upon the direction of heat flow (body to boundary layer or boundary layer to body) and the magnitude of heat flow. The desirable condition of zero heat transfer for the elimination of heat-transfer effects could not be achieved due to the relatively short running periods of the blowdown tunnel with atmospheric supply conditions.

Since the Reynolds number per unit length decreased with increasing Mach number (atmospheric supply conditions) it was also necessary to increase the sphere size and consequently the heat capacity of the sphere with increasing Mach number in order to establish a certain Reynolds number (referred to sphere diameter) for the whole Mach number range. A qualitative survey showed that at a considered constant Reynolds number the variation of sphere heat capacity with Mach number at Mach numbers from 1.57 to 3.26 was negligible as compared to the considerable increase in heat capacity at Mach numbers of 4.24 and 5.00. It was therefore concluded that there was a unique approach - even though not complete - to equilibrium temperature conditions and consequently no relative heat-transfer influence at Mach numbers up to M = 3.26. However, at Mach numbers of 4.24 and 5.00 - still considering a certain Reynolds number - the higher heat capacities (several orders of magnitude) of the spheres must have retained heat-flow conditions from the wall into the boundary layer and mixing zones which are comparable with those of heated cone-cylinder models. Heating of models tends to increase the base pressure as reported by H. H. Kurzweg in reference (1).

13. It was necessary to obtain information on the base-pressure distribution in order to calculate the magnitude of the base-drag coefficient as compared to the total-drag coefficient. It was already known from pressure distribution measurements on a 4 cm sphere carried out at several Mach numbers by S. Erdmann at Peenemuende, Germany (m) that the pressure is constant beyond the flow separation point. Therefore, there was certain evidence that the base pressure could be applied to the sphere surface beyond the separation point for the calculation of the base-drag coefficient. The location of the separation point was determined from schlieren photographs. Figures 4a and 4b show some examples of spark-schlieren photographs at M = 3.26. The base-drag coefficient C_{D_b} is plotted in Figure 8 vs. Reynolds number with the parameter of the Mach number. Corresponding to the decrease of base pressure in the Reynolds number region considered, one finds here an increase of the base-drag coefficient up to a region of constant behavior. In this connection it should be remarked that the supersonic flow separation (laminar separation) was generally observed at angles $> 90^{\circ}$ referred to the stagnation point. This observation is in agreement with results from firing tests carried out at Aberdeen by A. C. Charters and R. N. Thomas (e). A slight increase of the separation angle by a few degrees (max. 4°) with increasing Reynolds number could be

detected as a general tendency at all Mach numbers. However, the Mach number effect is predominant up to $M = 3.26$. Observed extreme data of the separation angle were 92^o at $M = 1.57$ and 101^o at $M = 3.26$ and $M = 4.24$. The measured separation angle of about 100^o at $M = 1.88$ and $Re = 5.5 \times 10^5$ is in good agreement with the separation location taken from Erdmann's pressure distribution (m). It might be recalled that subcritical (laminar) and supercritical (turbulent) separation angles at incompressible subsonic speeds were found to be 80^o and 110^o, respectively (a). This obvious difference between subsonic and supersonic behavior is certainly due to the effect of pressure gradients. Only subcritical (laminar) separation could be compared since supercritical (turbulent) separation has not been produced as yet at supersonic speeds.

14. For the purpose of comparison of the drag components the wave-drag coefficient of the sphere was calculated at Mach numbers of 1.88, 2.48, 3.24 and 4.24. A method developed by M. M. Munk and J. C. Crown at NOL was used for this calculation (n). The method assumes the knowledge of the shape of the head shock wave over a sufficient length in flow direction. The results are plotted vs. Mach number in Figure 9 together with a region of variation of the base-drag coefficient determined by the Reynolds number effect ($0.06 \times 10^6 \leq Re \leq 1.4 \times 10^6$) and an average curve of Goettingen (c) and Peenemuende (d) total-drag coefficients. The increase of the wave-drag coefficient with increasing Mach number is compensated by the decrease of the base-drag coefficient. This fact explains the nearly constant behavior of the total-drag coefficient. The maximum base-drag coefficient amounts to 32 per cent of the total-drag coefficient at $M = 1.57$ and 3 per cent at $M = 4.24$. It is not surprising that previous investigations in wind tunnels could not detect any Reynolds effect at supersonic speeds in the considered Reynolds number region since only total force measurements were used to determine the total-drag coefficient whose variation due to the Reynolds effect on the base-drag coefficient ranged within the measuring accuracy. In the case of measuring equipment available to the author at that time, this accuracy was ± 5 per cent. Absolute measuring accuracies from 0.015 to 1.5 grams would be necessary to detect this effect by total-drag measurements in the NOL wind tunnels with atmospheric supply conditions in the considered region of Mach and Reynolds numbers. In this connection it must be mentioned that A. May and W. R. Witt, Jr. could detect a slight increase of the total-drag coefficient with increasing Reynolds number in the Reynolds number region

$10^5 \leqq Re \leqq 2 \times 10^6$ at all Mach numbers from M = 2 to M = 3.4 during their recent free-flight determinations of the drag coefficient of spheres in the NOL Pressurized Ballistics Range (reference j).

CONCLUSIONS

15. It was shown from base-pressure measurements on spheres at supersonic speeds that the base-pressure component of the total-drag coefficient is a function of the Reynolds number and that it can be affected by boundary-layer disturbances. The estimated Reynolds number effect on the total-drag coefficient in the considered Reynolds number region ($10^5 \leqq Re \leqq 10^6$) is very small (max. 10 per cent at M = 1.57, min. 1 per cent at M = 4.24). Therefore, high accuracy is required for the determination of Reynolds number effect on the total-drag coefficient by total force measurements. The effects of Mach number on wave- and base-drag coefficients cancel each other. Consequently, the total-drag coefficient is almost independent of Mach number. The good agreement between wake configurations determined from wind-tunnel schlieren photographs and firing-range shadowgraphs at corresponding Mach numbers and Reynolds numbers encourages the extension of comparative tests with spheres to higher Reynolds numbers in both, the wind tunnel and the firing range. The desirable condition to be established will be the case of turbulent separation in order to have a complete comparison between subsonic and supersonic flow separation phenomena. The failure to detect a critical Reynolds number for spheres at supersonic speeds might be explained by the fact that turbulent separation could not be obtained if one assumes that supersonic, turbulent separation causes a similar effect as known from subsonic investigations. Pressure and temperature probe surveys in the wake would help to obtain experimentally a more complete picture of the wake and mixing flow mechanism.

REFERENCES

(a) Wien-Harms, "Handbuch der Experimental-Physik IV, 2, Hydro-und Aerodynamik", Chapter IV, § 13

(b) Eula, A., "L'Influenca del numero di Reynolds ai grandi numeri di Mach", L'Aerotechnica, Vol. XX (1940). No. 1, pp. 20/29

(c) Walchner, O., "Systematische Geschossmessungen im Windkanal", AVA report 41/8/6, Goettingen.

(d) Lehnert, R., "Dreikomponentenmessungen an Kugeln im Ueberschall", Peenemuende archive report 66/46, 1942 or "Systematische Messungen an neun einfachen Geschossformen im Vergleich zu Messungen der AVA Goettingen", Lilienthal-Gesellschaft fuer Luftfahrtforschung Bericht 139, 2. Teil 1941.

(e) Charters, A. C. and Thomas, R. N., "The Aerodynamic Performance of Small Spheres from Subsonic to High Supersonic Velocities", Journal of Aeronautical Sciences, 1945, p. 468

(f) Lightfoot, J. R., "The Naval Ordnance Laboratory Aeroballistic Research Facility", NOLR 1079, August 1950

(g) Kurzweg, H. H., "Interrelationship between Boundary Layer and Base Pressure", Journal of Aeronautical Sciences, 1951, p. 743

(h) Chapman, Dean, R., "An Analysis of Base Pressure at Supersonic Velocities and Comparison with Experiment", NACA TN 2137, 1950

(i) Bogdonoff, S. M., "A Preliminary Study of Reynolds Number Effect on Base Pressure at M = 2.95", Journal of Aeronautical Sciences, 1952, p. 201

(j) May, A. and Witt, W. R. Jr., "Free-Flight Determination of the Drag Coefficient of Spheres, NAVORD Report 2352, 14 August 1952

(k) Crocco, L. and Lees, L., "A Mixing Theory for the Interaction Between Dissipative Flows and Nearly Isentropic Streams", Journal of Aeronautical Sciences, 1952, p. 649

(l) Kurzweg, H. H., "The Base Pressure Measurements of Heated, Cooled, and Boat-tailed Models at Mach Numbers 1.5 to 5.0, Bureau of Ordnance Committee on Aeroballistics Symposium, Austin, Texas, Nov. 16 - 17, 1950

(m) Erdmann, S., "Widerstand von Kegeln und Kugeln aus der Druckverteilung bei Ueberschallgeschwindigkeit", Lilienthal-Gesellschaft fuer Luftfahrtforschung Bericht 139, 2 Teil 1941

(n) Munk, M. M. and Crown, J. C., "The Head Shock Wave, NOLM 9773, 25 August 1948

APPENDIX

Support effect investigations

(1) Effect of sting inclination.

Some base-pressure measurements at M = 2.48 were carried out with variation of the angle of attack of the sting support ($-6 \leqq \alpha \leqq +9^{o}$). The center of rotation of the α - mechanism coincided with the sphere center in all cases tested. (Figure 1) The results presented as base pressure ratio vs. sting inclination in Figure 10 show that small deviations from $\alpha = 0$ do not cause any measurable defects in general. However, larger sting inclination of larger spheres affects the base pressure. The increase of the base-pressure ratio with increasing sting inclination is accompanied by an upstream travel of the trailing shock emanating from the intersection of wake boundary and inclined sting.

(2) Effect of relative frontal sting area.

At the beginning of the base-pressure measurements it was thought to be worthwhile to study the effect of relative sting thickness. This was done simply by replacing the tare-sting (Figure 1) by a thin copper tubing for picking up the base pressure at Mach number M = 1.88. The results of the comparison tests with and without tare-sting are plotted as base-pressure ratio vs. Reynolds number (Figure 11). The absence of the tare sting did not change considerably the base-pressure tendency as found with the split-sting support. However, since the small effect found was a systematic one and since it was felt that the reduced sting frontal area represented an experimental condition closer to the no sting condition it was decided to use only the data obtained without tare-sting at M = 1.88 and to carry out the whole investigation without tare-sting at the other Mach numbers also.

In general, the conclusion can be drawn that caution must be exercised if force measurements are carried out with a split-sting support system unless the base pressure is properly measured and deducted.

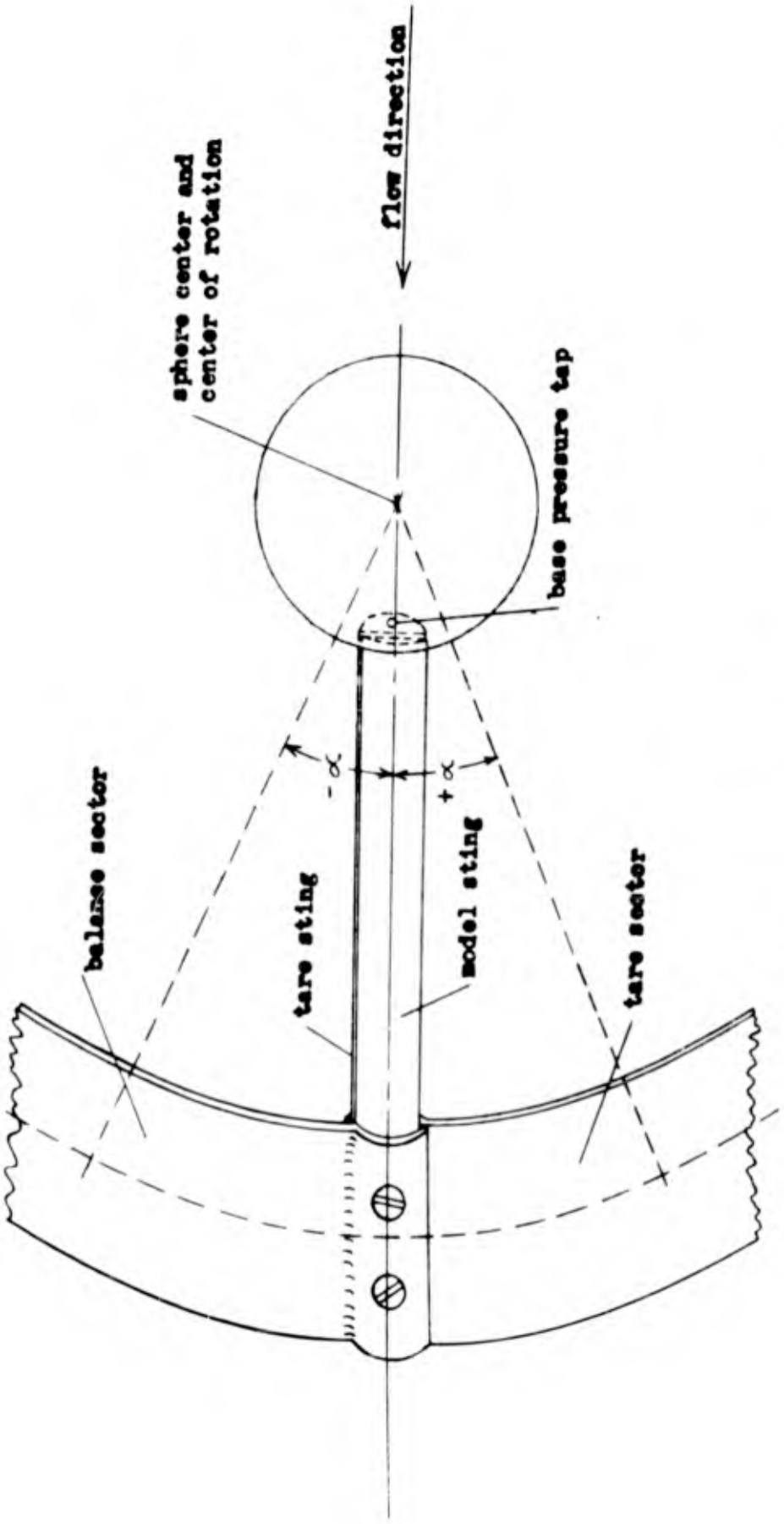

Figure 1 - Schematic sketch of sphere support

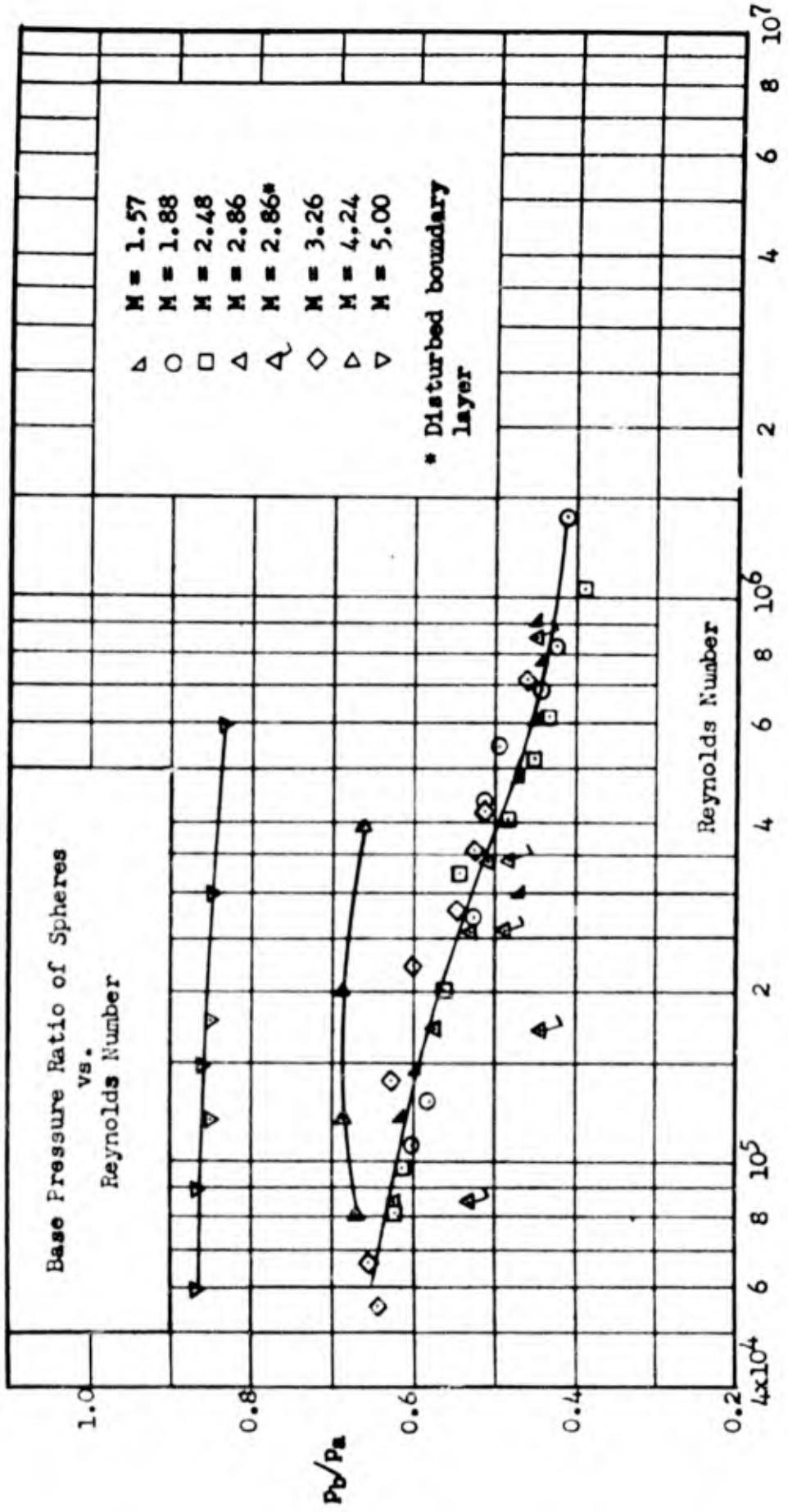

Figure 2 - Base pressure ratio of spheres vs. Reynolds number

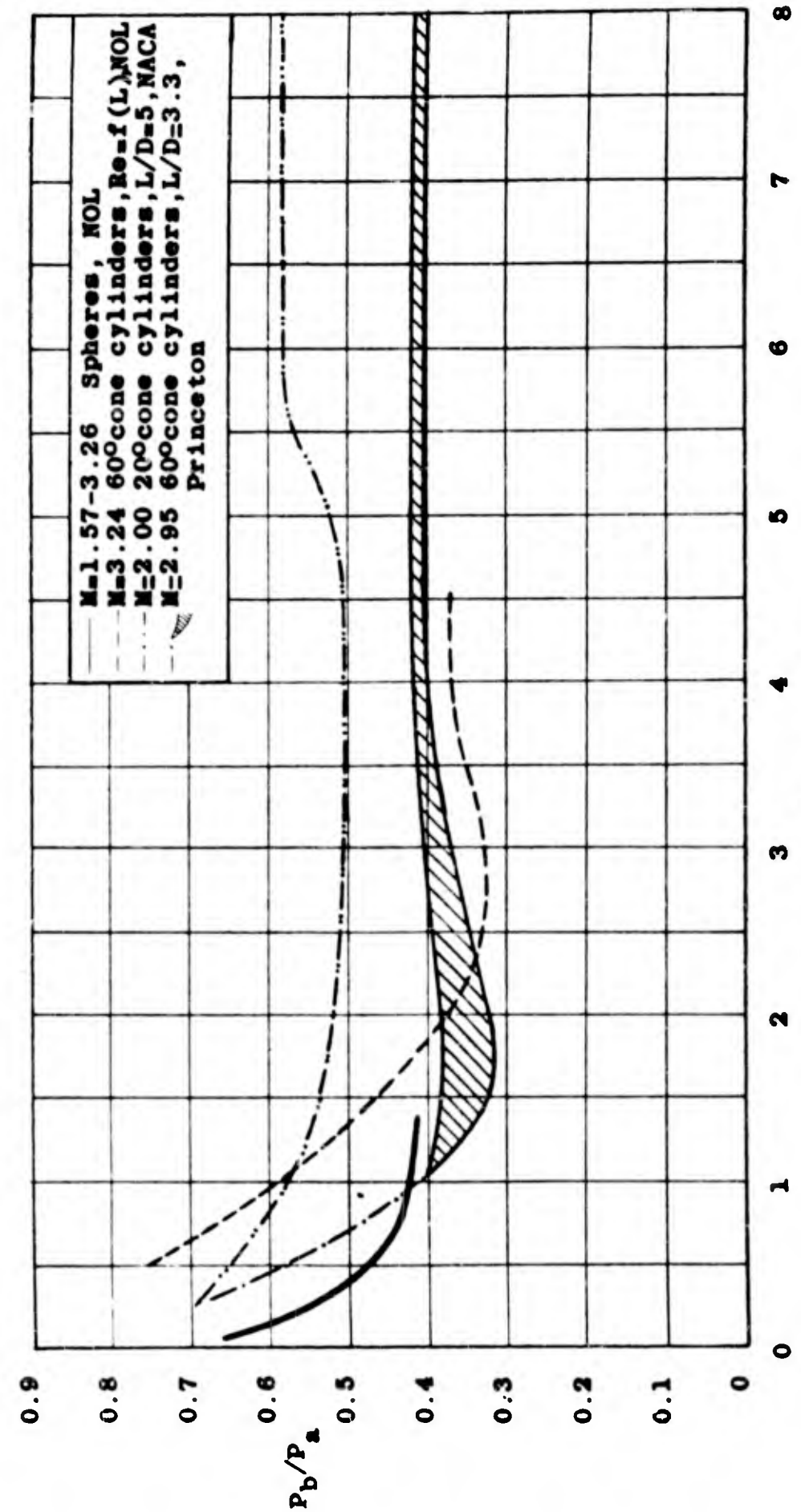

Figure 3 - Average base pressure ratio of spheres and cone cylinders vs. Reynolds number

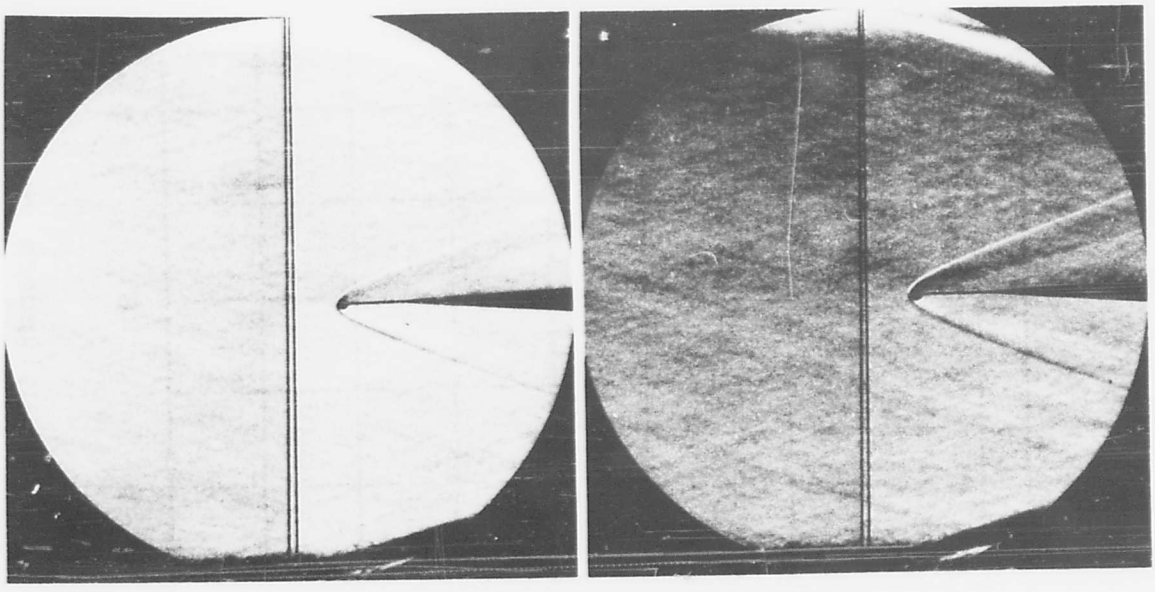

0.7925 cm Diameter

0.9515 cm Diameter

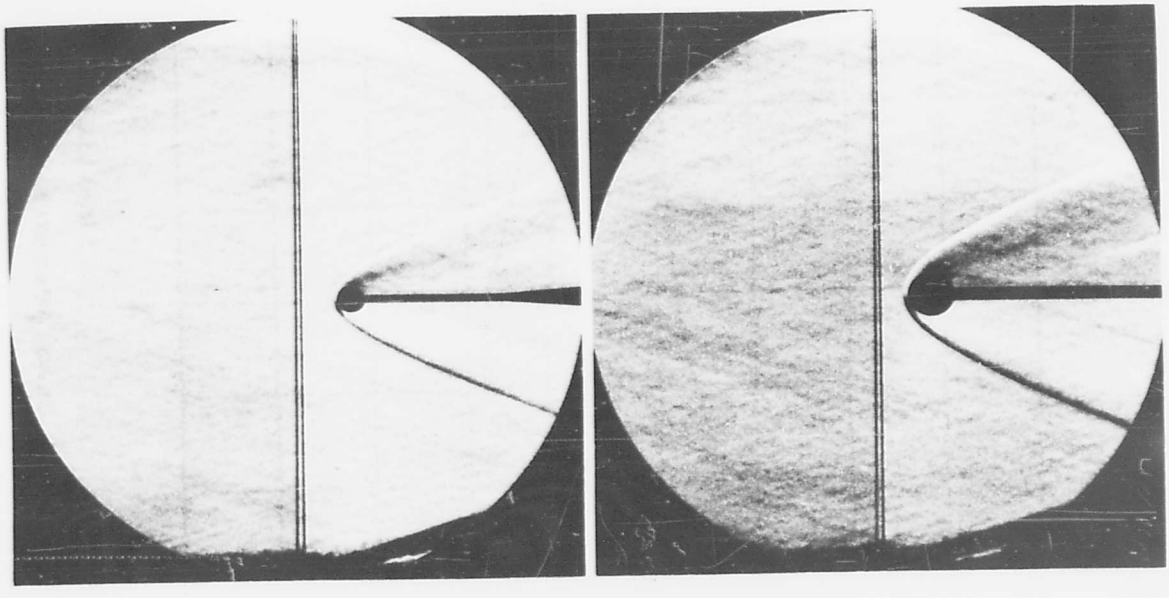

1.977 cm Diameter

3.170 cm Diameter

Figure 4a - Schlieren photographs of spheres at M = 3.26

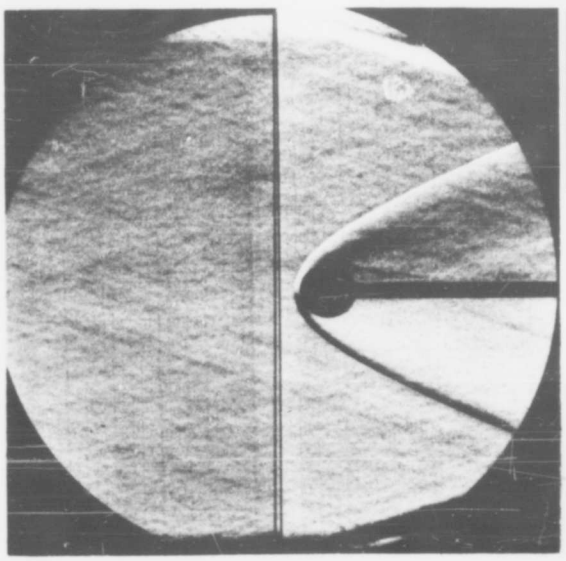

3.959 cm Diameter

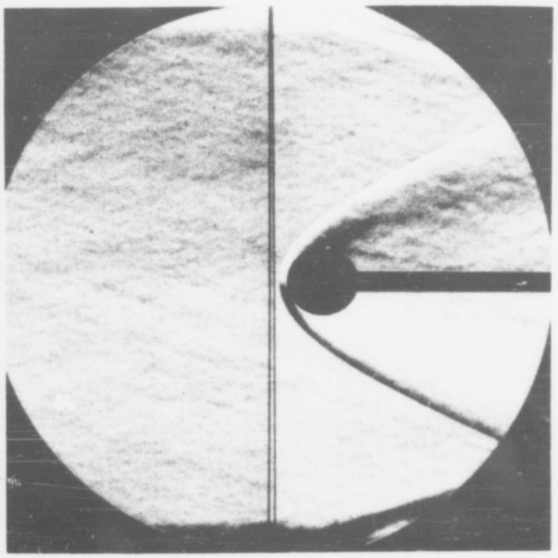

5.048 cm Diameter

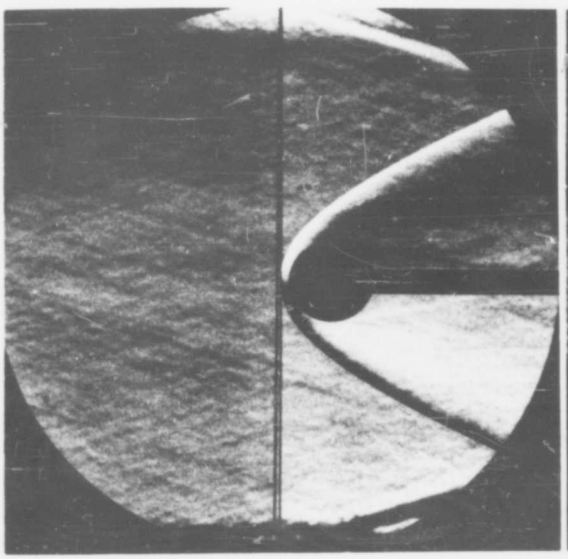

5.972 cm Diameter

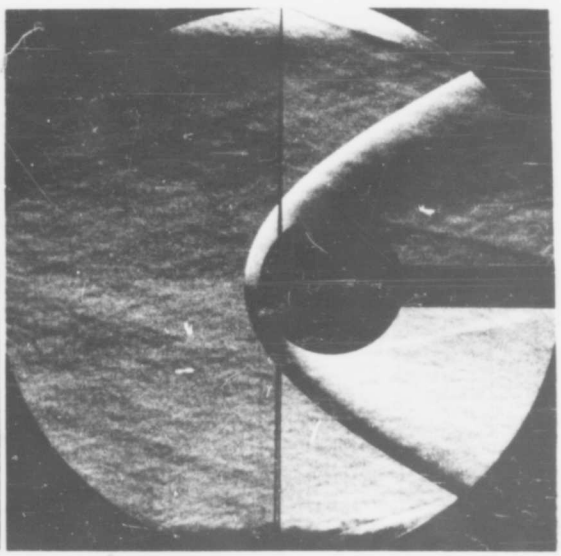

10.146 cm Diameter

Figure 4b - Schlieren photographs of spheres at M = 3.26 (continued)

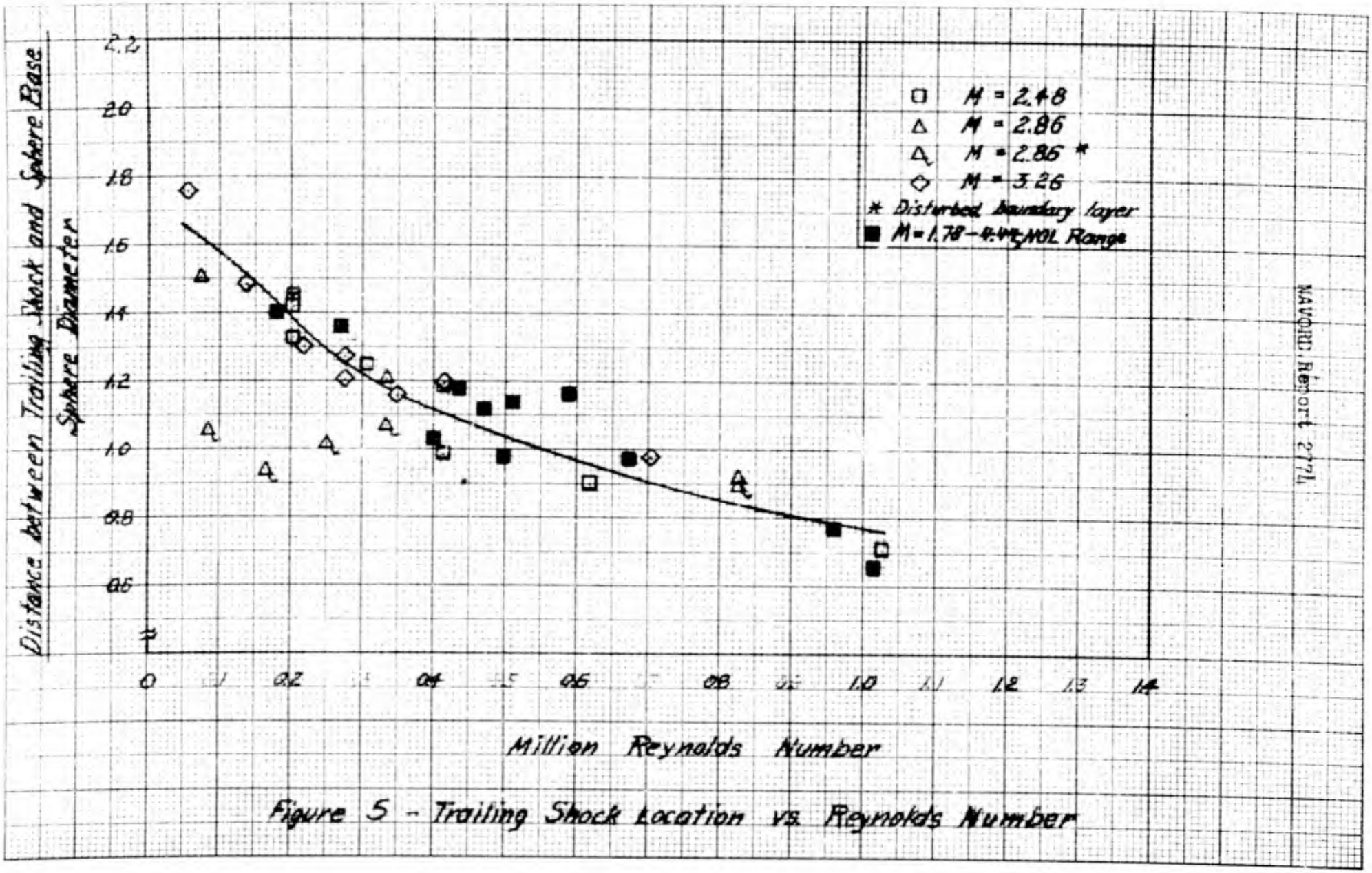

Figure 5 - Trailing Shock Location vs. Reynolds Number

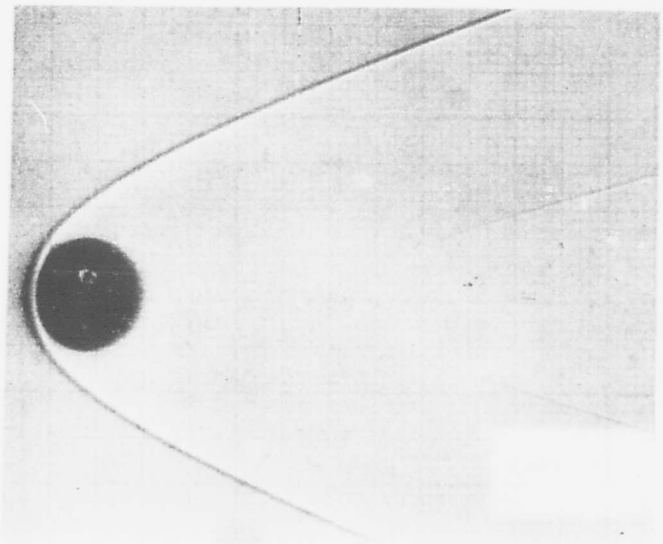

Re = 0.437×10^6

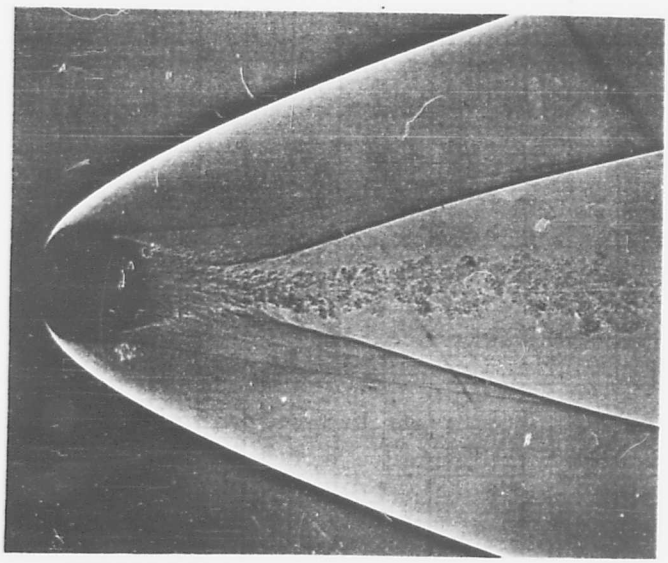

Re = 1.013×10^6

Figure 6 - Shadowgraphs of spheres at M~4

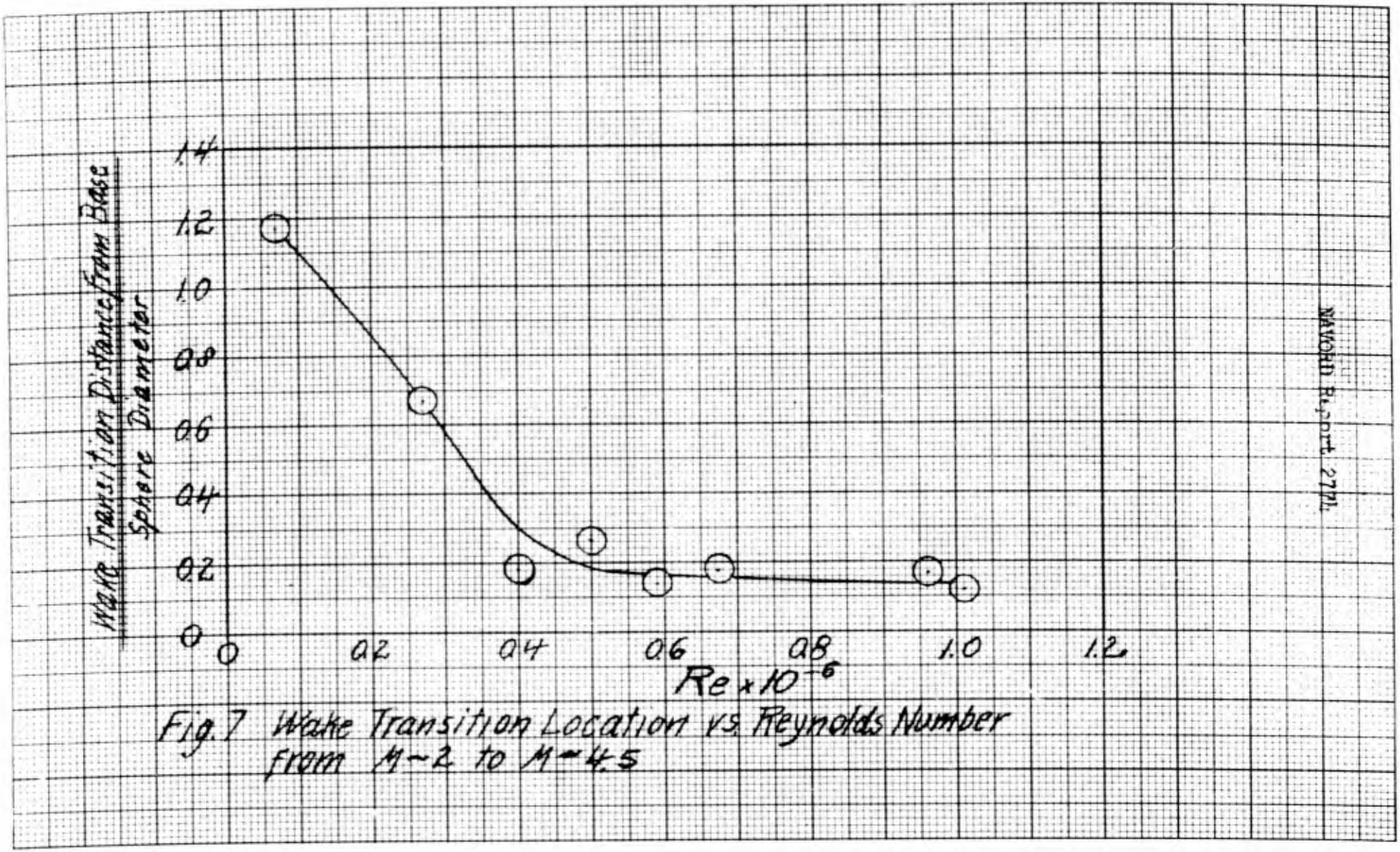

Fig. 7 Wake Transition Location vs. Reynolds Number from M=2 to M=4.5

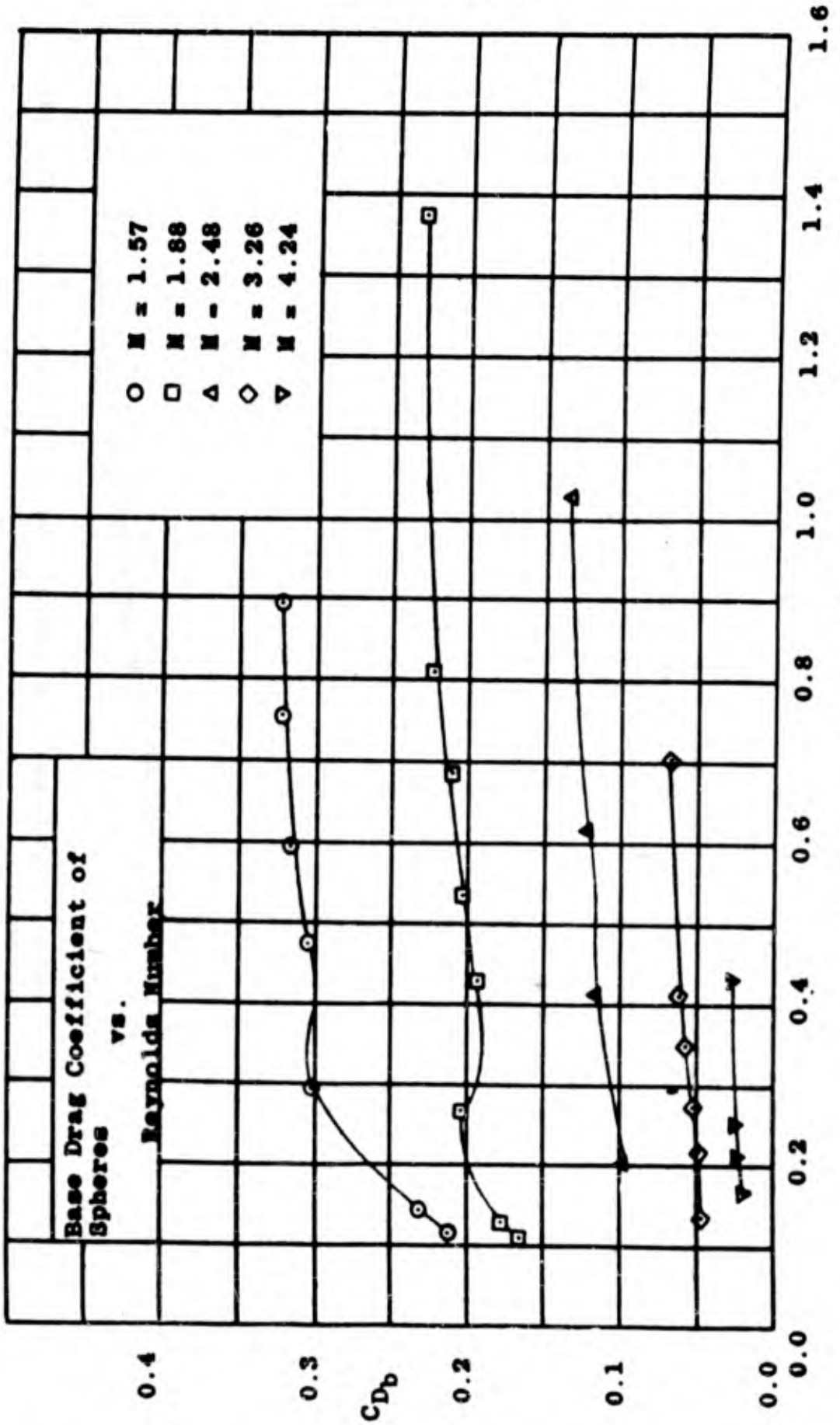

Figure 8 - Base drag coefficient of spheres vs. Reynolds number

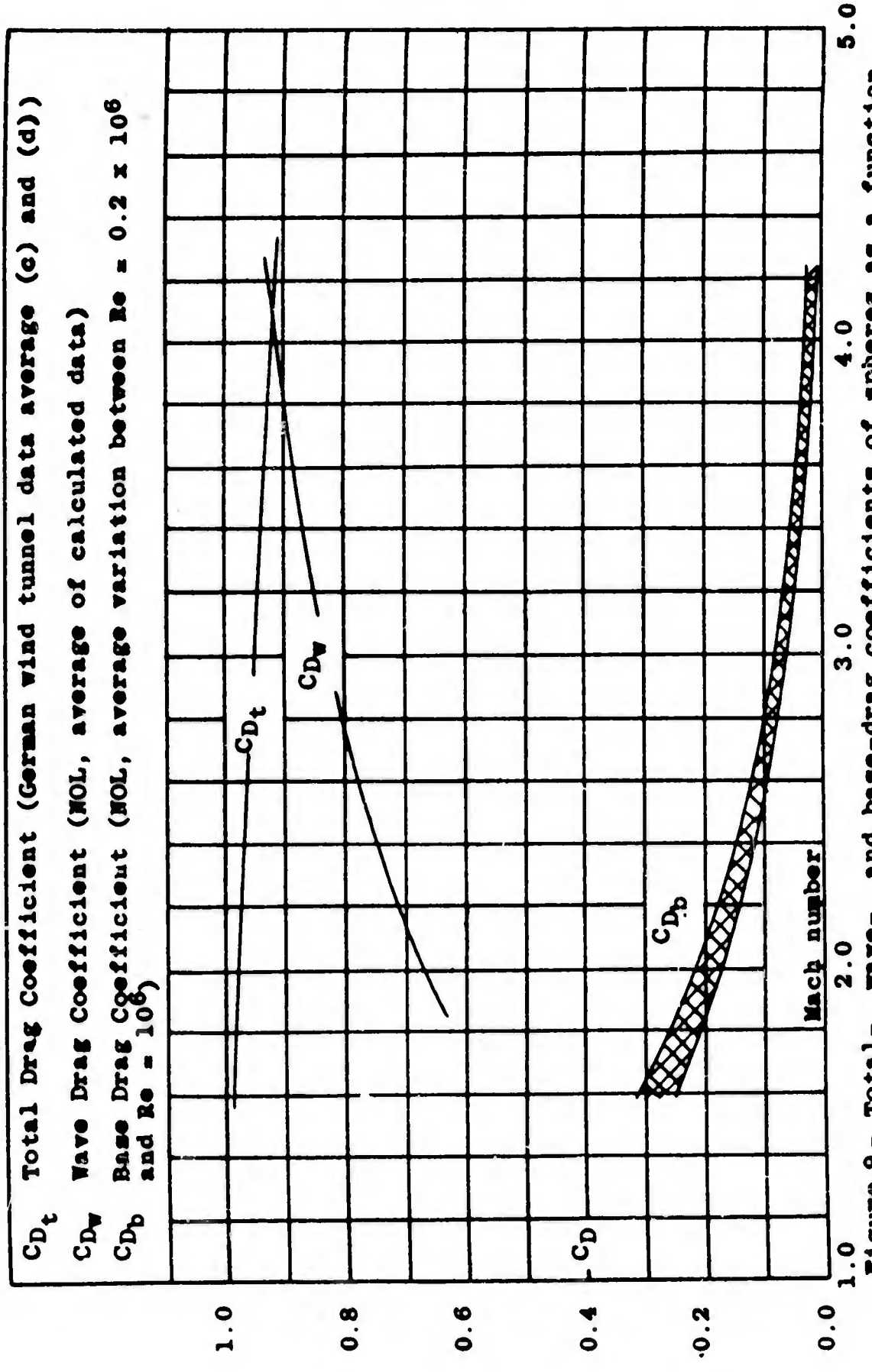

Figure 9 - Total-, wave-, and base-drag coefficients of spheres as a function of Mach number.

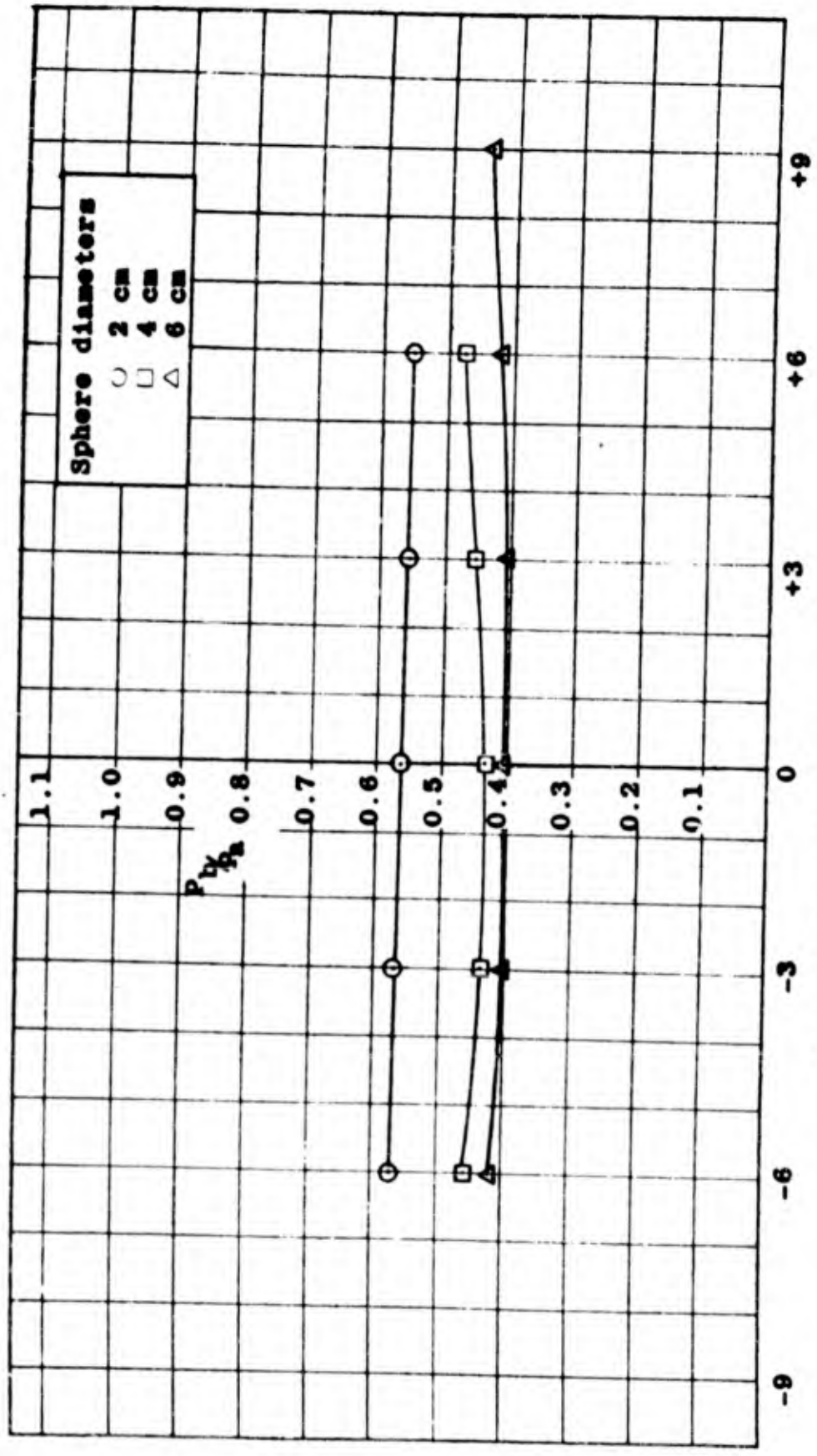

Figure 10—Effect of sting inclination on base pressure ratio of spheres at M = 2.48

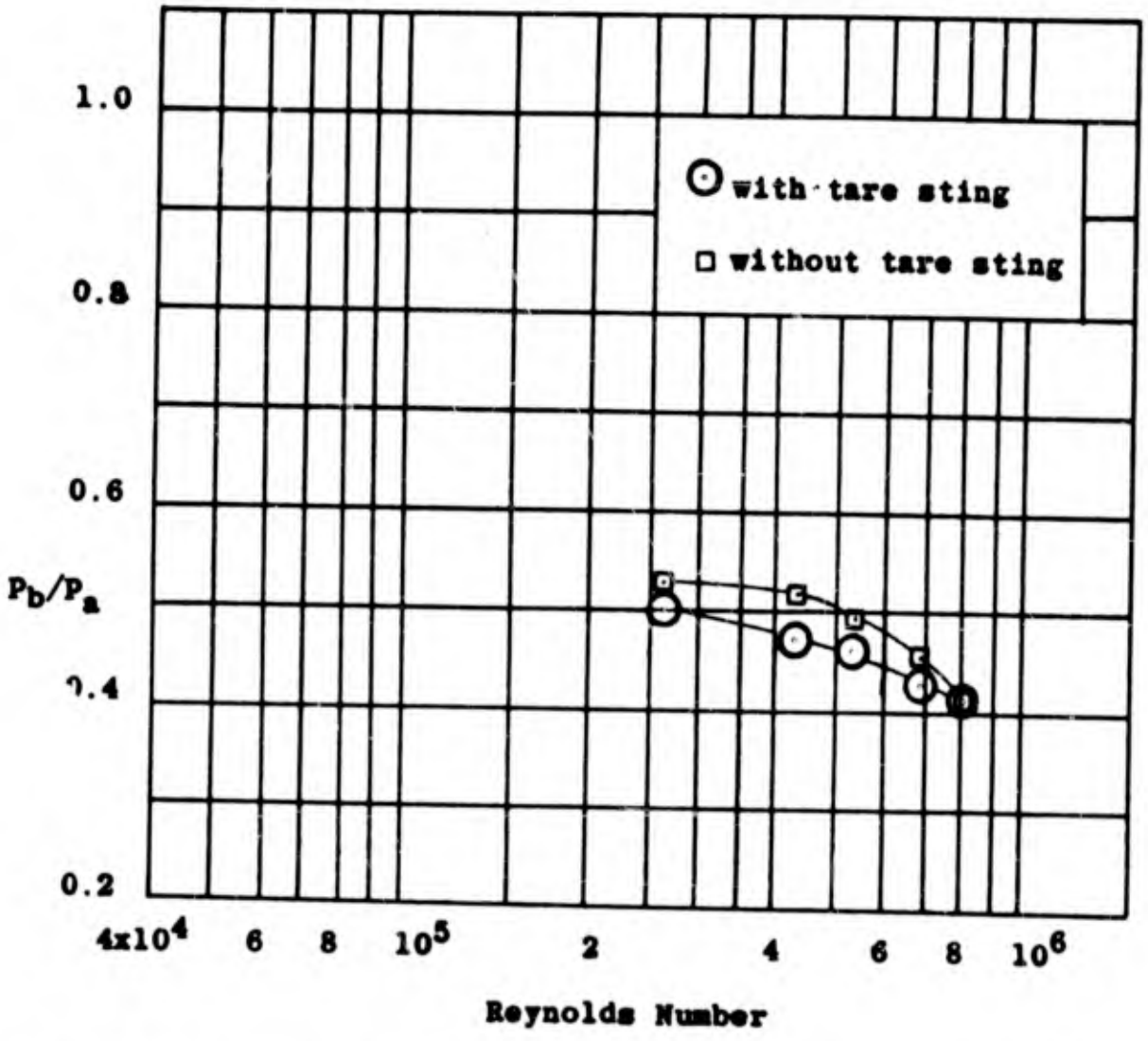

Figure 11 - Sting effect on base pressure ratio of spheres at M = 1.88.

Aeroballistic Research Department
External Distribution List for Development (X2)

No. of Copies	
	Chief, Bureau of Ordnance Department of the Navy Washington 25, D. C.
1	Attn: Rea
1	Attn: Rexe
1	Attn: Re3d
3	Attn: Re9a
	Chief, Bureau of Aeronautics Department of the Navy Washington 25, D. C.
1	Attn: AER-TD-414
2	Attn: RS-7
	Commander U.S. Naval Ordnance Test Station Inyokern P.O. China Lake, California
2	Attn: Technical Library
	Commander U.S. Naval Air Missile Test Center Point Mugu, California
3	Attn: Technical Library
	Superintendent U.S. Naval Postgraduate School Monterey, California
1	Attn: Librarian
	Commanding Officer and Director David Taylor Model Basin Washington 7, D. C.
1	Attn: Hydrodynamics Laboratory
	Chief of Naval Research Navy Research Section Library of Congress
2	Washington 25, D. C.
	Chief, Naval Operations Department of the Navy Washington 25, D. C.
1	Attn: Op-51
	Office of Naval Research Department of the Navy Washington 25, D. C.
2	Attn: Code 463
	Director Naval Research Laboratory Washington 25, D. C.
1	Attn: Code 2021 Code 3800
	Officer-in-Charge Naval Aircraft Torpedo Unit U.S. Naval Air Station
1	Quonset Point, Rhode Island
	Office, Chief of Ordnance Washington 25, D. C.
1	Attn: ORDTU

No. of Copies	
	Research and Development Board Library Branch Pentagon 3D1041
2	Washington 25, D. C.
	Chief, AFSWP P.O. Box 2610 Washington, D. C.
1	Attn: Technical Library
	Chief, Physical Vulnerability Branch Air Targets Division Directorate of Intelligence Headquarters, USAF
1	Washington 25, D. C.
	The Artillery School Antiaircraft and Guided Missiles Br. Fort Bliss, Texas
2	Attn: Research and Analysis Sec.
	Commanding General Wright Air Development Center Wright-Patterson Air Force Base Dayton, Ohio
8	Attn: WCAPD
2	Attn: WCRR
1	Attn: WCSD
5	Attn: WCSO
	Director Air University Library
1	Maxwell Air Force Base, Alabama
	Commanding General Aberdeen Proving Ground Aberdeen, Maryland
1	Attn: C.L. Poor
	National Bureau of Standards Washington 25, D. C.
1	Attn: Librarian (Ord. Dev. Div.)
1	Attn: W. Ramberg
	National Bureau of Standards Corona Laboratories (Ord.Dev.Div.) Corona, California
1	Attn: Dr. H. Thomas
	National Bureau of Standards Building 3U, UCLA Campus 405 Hilgard Avenue Los Angeles 24, California
1	Attn: Librarian
	University of California Berkeley 4, California
1	Attn: Mr. G. J. Maslach
1	Attn: Dr. S. A. Schaaf
	California Inst. of Technology Pasadena 4, California
2	Attn: Librarian(Guggenheim Aero. Lab.) VIA: BuAero

No. of Copies

University of Michigan
Willow Run Research Center
Ypsilanti, Michigan
1 Attn: L.R. Biasell
VIA: InsMat

University of Minnesota
Rosemount, Minnesota
1 Attn: J. Leonard Frame
VIA: Ass't InsMat

The Ohio State University
Columbus, Ohio
1 Attn: G.L. VonEschen
VIA: Ass't InsMat

Polytechnic Institute of Brooklyn
99 Livingston Street
Brooklyn 2, New York
1 Attn: Dr. Antonio Ferri
VIA: ONR Branch Office

Princeton University
Forrestal Research Center Library
Project Squid
1 Princeton, New Jersey

Massachusetts Inst. of Technology
Project Meteor
Cambridge 39, Massachusetts
2 Attn: Guided Missiles Library

Applied Physics Laboratory
The Johns Hopkins University
8621 Georgia Avenue
Silver Spring, Maryland
1 Attn: Arthur G. Norris
Technical Reports Office
VIA: NIO

Armour Research Foundation
35 West 33rd Street
Chicago 16, Illinois
1 Attn: Engr. Mechanics Division
VIA: ONR Branch Office

Defense Research Laboratory
University of Texas
Box 1, University Station
1 Austin, Texas
VIA: InsMat

Eastman Kodak Company
Navy Ordnance Division
50 West Main Street
Rochester 4, New York
2 Attn: Dr. Herbert Trotter, Jr.
VIA: NIO

No. of Copies

General Electric Company
Building #1, Campbell Avenue Plant
Schenectady, New York
1 Attn: J.C. Hoffman
VIA: InsMachinery

The Rand Corporation
1500 Fourth Street
Santa Monica, California
1 Attn: The Librarian
VIA: InsMat

Consolidated Vultee Corporation
Daingerfield, Texas
1 Attn: J.E. Arnold, Manager
VIA: Dev. Contract Office

Douglas Aircraft Company, Inc.
3000 Ocean Park Boulevard
Santa Monica, California
1 Attn: Mr. E.F. Burton
VIA: BuAero Resident Rep.

North American Aviation, Inc.
12214 Lakewood Boulevard
Downey, California
2 Attn: Aerophysics Laboratory
VIA: BuAero Rep.

National Advisory Committee for Aero.
1724 F Street Northwest
Washington 25, D. C.
5 Attn: Mr. E. B. Jackson

Ames Aeronautical Laboratory
Moffett Field, California
1 Attn: H. Julian Allen
2 Attn: A.C. Charters

Theoretical Aerodynamics Division
Langley Aeronautical Laboratory
Langley Field, Virginia
1 Attn: Theoretical Aerodynamics Div.
1 Attn: Dr. A. Busemann
2 Attn: J. Steele

NACA Lewis Flight Propulsion Lab.
Cleveland Hopkins Airport
Cleveland, Ohio
1 Attn: Dr. John C. Evvard

Hughes Aircraft Company
Culver City, California
1 Attn: Dr. Allen E. Puckett

Institute of Aerophysics
University of Toronto
Toronto 5, Ontario
1 Attn: Dr. Gordon N. Patterson, Dir.
VIA: BuOrd (Ad8)

Aeroballistic Research Department
External Distribution List for Aeroballistics Research (XIa)

No. of Copies	
6	Office of Naval Research Branch Office Navy 100 Fleet Post Office New York, New York
	Commanding General Aberdeen Proving Ground Aberdeen, Maryland
1	Attn: Dr. B.L. Hicks
	National Bureau of Standards Aerodynamics Section Washington 25, D.C.
1	Attn: Dr. G.B. Schubauer, Chief
	Ames Aeronautical Laboratory Moffett Field, California
1	Attn: Walter G. Vincenti
	University of California Observatory 21 Berkeley 4, California
1	Attn: Leland E. Cunningham VIA: InsMat
	Massachusetts Inst. of Technology Dept. of Mathematics, Room 2-270 77 Massachusetts Avenue Cambridge, Massachusetts
1	Attn: Prof. Eric Reissner VIA: InsMat
	Graduate School Aeronautical Engr. Cornell University Ithaca, New York
1	Attn: W.R. Sears, Director VIA: ONR
	Applied Math. and Statistics Lab. Stanford University Stanford, California
1	Attn: R.J. Langle, Associate Dir. VIA: Ass't InsMat
	University of Minnesota Dept. of Aeronautical Engr. Minneapolis, Minnesota
1	Attn: Professor R. Hermann VIA: Ass't InsMat
	Case Institute of Technology Dept. of Mechanical Engineering Cleveland, Ohio
1	Attn: Professor G. Kuerti VIA: ONR
	Harvard University 109 Pierce Hall Cambridge 38, Massachusetts
1	Attn: Professor R. von Mises

Aeroballistic Research Department
External Distribution List for Aeroballistics Research

No. of Copies		No. of Copies	
1	Dr. F. D. Bennett Exterior Ballistics Laboratory Aberdeen Proving Ground Aberdeen, Maryland	1	Dr. E. R. Van Driest Aerophysics Laboratory North American Aviation, Inc. Downey, California
1	Professor J. F. Ludloff New York University Aeronautics Department University Heights, New York 53, New York		
1	Dr. Henry T. Nagamatsu, Director Hypersonic Wind Tunnel Guggenheim Aeronautical Laboratory California Institute of Technology Pasadena 4, California		
	Princeton University Jet Propulsion Center		
1	Attn: Prof. L. Crocco		
1	Attn: Prof. L. Lees		
	Defense Research Laboratory University of Texas Box 1, University Station Austin, Texas		
1	Attn: Dr. M. J. Thompson Via: InsMat		
1	Dr. G. R. Eber Holloman Air Force Base Alamogordo, New Mexico		
1	Dr. Peter P. Wegener Jet Propulsion Laboratory 4800 Oak Grove Drive Pasadena, California		
1	Mr. J. L. Potter Technical & Engineering Division 98 Caldwell Road Redstone Arsenal Huntsville, Alabama		